

# Resonant x-ray scattering at the Se edge in liquid crystal free-standing films and devices

L. S. Matkin, H. F. Gleeson<sup>a)</sup>

*Department of Physics and Astronomy, Manchester University, Manchester M13 9PL, United Kingdom*

P. Mach and C. C. Huang

*School of Physics and Astronomy, University of Minnesota, Minnesota 55455*

R. Pindak

*Lucent Technologies, Bell Laboratories, Murray Hill, New Jersey*

G. Srajer and J. Pollmann

*APS, Argonne National Laboratory, Argonne, Illinois 60439*

J. W. Goodby, M. Hird, and A. Seed

*Department of Chemistry, Hull University, Hull HU6 7RJ, United Kingdom*

(Received 6 December 1999; accepted for publication 31 January 2000)

Resonant x-ray diffraction was carried out at the Se *K* edge in thick free-standing films of a selenophene liquid crystalline material, revealing detail of the structure of the ferro-, ferri-, and antiferroelectric phases. The ferrielectric phase was shown to have a three-layer superlattice. Moreover, the structure of a lower temperature hexatic phase was established. For the antiferroelectric phase, investigations were also carried out in a planar device configuration. The device allowed resonant scattering experiments to be carried out with and without the application of an electric field and resonant data are compared with electro-optic measurements carried out on the same device. © 2000 American Institute of Physics. [S0003-6951(00)01513-8]

The rapid, tristable switching<sup>1</sup> of antiferroelectric liquid crystals<sup>2</sup> has been responsible for the recent interest in their application to display devices<sup>3</sup> and optical elements such as spatial light modulators. The properties of the more complex ferrielectric<sup>4</sup> phases are far less well understood and their structure has been the subject of considerable controversy. Several models have been proposed for the ferrielectric phases.<sup>4-6</sup> In general the liquid crystal ferroelectric, ferrielectric, and antiferroelectric phases (smectic C\* subphases) are formed from rod-like molecules arranged in a layered structure. The molecules are chiral and have an average molecular direction (the director) tilted with respect to the layer normal. The particular orientation of the director with respect to adjacent layers defines the specific subphase. Recently the clock model<sup>6</sup> has been shown to agree with the structure of the ferri phases in certain sulfur containing compounds using x-ray resonant scattering combined with polarization analysis.<sup>7,8</sup>

The structures of the smectic-C\* (SmC\*) subphases have been investigated primarily indirectly, using techniques such as electro-optic and polarization measurements, dielectric spectroscopy, conventional x-ray scattering and microscopy. Resonant scattering allows the direct investigation of the director orientation within smectic layers,<sup>7</sup> and is particularly useful in the elucidation of structural information in the SmC\* subphases. Understanding the details of the antiferro- and ferrielectric structures is an important step toward optimizing their potential for device applications. In this letter the application of resonant scattering to a selenium contain-

ing liquid crystal compound is reported, studying the detailed structure of the SmC\* subphases. Scattering is carried out on thick free-standing films and resonant signals are also detected in a device geometry with the application of electric fields, enabling field induced structural changes to be studied.

The material used is a Se containing heterocyclic ester (AS620) with antiferroelectric and ferroelectric phases, together with one ferrielectric phase (Fig. 1). The physical properties of AS620 have been published elsewhere.<sup>9,10</sup>

The resonant x-ray scattering measurements were carried out at the 1-ID undulator beamline in the Advanced Photon Source, Argonne National Laboratory using an experimental arrangement similar to one described previously.<sup>8</sup> The free-standing film x-ray measurements were carried out in the specular Bragg scattering geometry. Conventional x-ray scattering produces peaks at  $Q_o = 2\pi/d$  and integral multiples of this value, where  $d$  is the smectic layer spacing. Conventional x-ray scattering probes only the average electron density of the material and provides no information on the detailed structures of the SmC\* subphases. However, scattering carried out in the resonant scattering regime is sensitive to

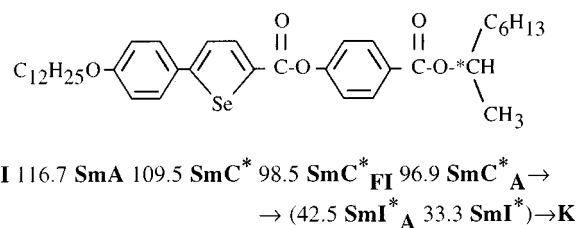


FIG. 1. The molecular structure and phase sequence of AS620.

<sup>a)</sup>Author to whom correspondence should be addressed; electronic mail: helen.gleeson@man.ac.uk

the relative director orientation.<sup>11</sup> Additional peaks are seen along  $Q_z/Q_o$ , the position and polarization of these peaks being determined by the substructure. Specifically, the clock model may be distinguished from the Ising model<sup>5</sup> by a polarization analysis of the resonant peaks.<sup>12</sup>

The SeK absorption edge in AS620 was determined prior to undertaking the resonant scattering experiments to be 12.658 keV and the x-ray beam was tuned to this energy.

Free-standing films of smectic liquid crystals provide an excellent layer arrangement. In these scattering experiments films were spread in the smectic-A phase (111 °C) to a thickness of approximately 200 smectic layers. The films were spread on a glass plate across a hole of dimension 5 mm×15 mm with gold electrodes along the two long edges, allowing the application of electric fields to the film. Temperature control was provided by a double oven that could be mounted on the x-ray beam line. Windows in the oven allowed *in-situ* observation of the film texture using a polarized microscope with a charge coupled device video camera. The film texture was observed during spreading and monitored throughout the experiment. The oven was mounted such that the x-ray beam scattered from the film at grazing incidence. Scans of scattered intensity as a function of  $Q_z/Q_o$  were carried out in the antiferroelectric, ferroelectric, ferrielectric SmC\* subphases as well as in a lower temperature hexatic phase. The resonant peaks obtained are shown in Fig. 2.

A polarization study of the scattered x-rays confirmed the clock model structure for the ferroelectric phase. As described in Ref. 12, in the clock model, the interlayer change in orientation for the SmC\* subphase molecules is a fixed angle with two contributions: a large rotation  $2\pi/\nu$  from the  $\nu$ -layer superlattice and a much smaller rotation  $2\pi\epsilon$ , where  $\epsilon$  is the ratio of the smectic layer spacing  $d$  to the optical pitch  $P_o$ . The different subphases exhibit different superlattice periodicities (values for  $\nu$ ). A helical clock structure results in resonant scattering peaks located at

$$Q_z/Q_o = \ell + m[(1/\nu) + \epsilon],$$

where  $\ell$  and  $m$  are integers and  $m=0, \pm 1$ , and  $\pm 2$ . In the ferroelectric SmC\* phase, there is no superlattice so the  $\nu$  dependence is removed from the equation. As shown in Fig. 2(a), the  $\ell=2$  layer peak has first order ( $m=\pm 1$ ) and second order ( $m=\pm 2$ ) resonant satellite peaks spaced apart by  $\epsilon$ . This scan was taken at  $T=104.2$  °C. From the measured  $d$  spacing,  $P_o$  can then be calculated for this phase to be 0.39  $\mu\text{m}$ . In the ferrielectric phase, one-third order resonant peaks were observed [Fig. 2(c)]. The peaks reveal that the ferrielectric phase has a three-layer superlattice. This contrasts with the four-layer superlattice observed in the sulfur analogue of this material.<sup>7</sup> In the antiferroelectric SmC\* phase, there is a two-layer superlattice ( $\nu=2$ ); and hence, a scan taken in this phase at 89.3 °C [Fig. 2(b)], exhibits half order peaks. The optical pitch causes these peaks to deviate from the exact half order position by  $\pm\epsilon$ . The measured splitting then allows us to determine the optical pitch as 0.58  $\mu\text{m}$ . Cooling into the hexatic phase, the half order peaks remained [Fig. 2(d)], indicating that this was also antiferroelectric; however, the split peaks merged, as the pitch increased with reducing temperature.

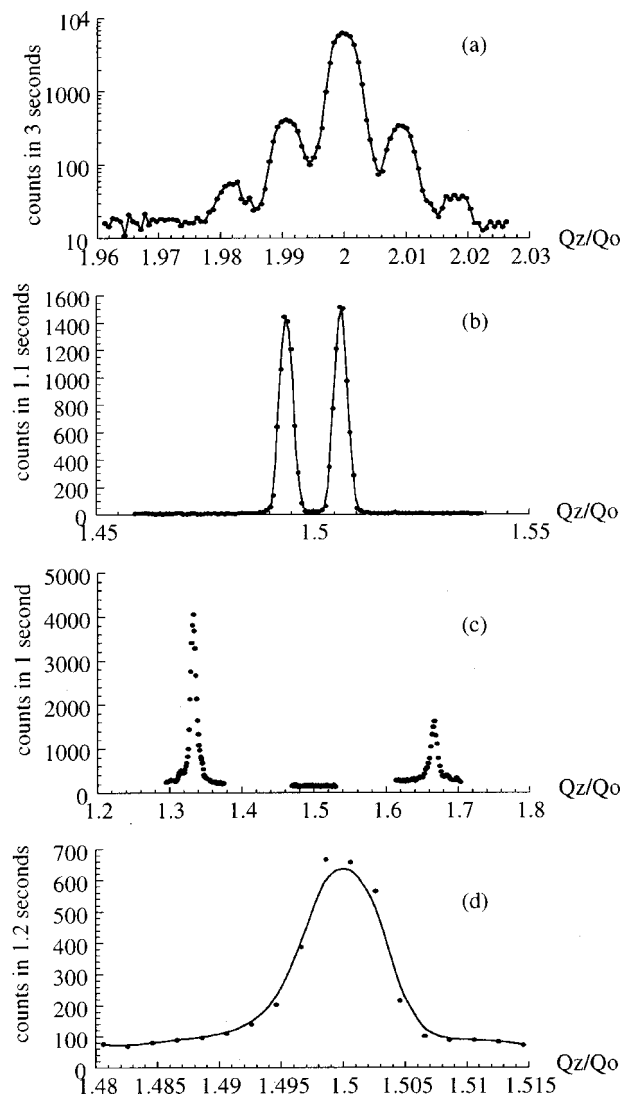


FIG. 2. X-ray intensity scans from thick free-standing films in the: (a) ferroelectric, (b) antiferroelectric, (c) ferrielectric SmC\* phases, and (d) of the lower temperature hexatic phase.

Having completed the structural characterization of the SmC\* subphases in free-standing films, we next attempted to observe resonant scattering from bulk samples in a device geometry. It is known that bulk materials can behave differently from free-standing films.<sup>13</sup> Further, the device geometry allows the application of large switching fields, a process which was found to be hindered in free-standing films due to the formation of ions in the film when x rays are incident on the sample. Ionic flow was evident in the film from the mobile textural changes observed when even very small fields were applied with x rays incident on the sample. The device cells consisted of two 300  $\mu\text{m}$  thick glass plates separated by a  $\sim 15$   $\mu\text{m}$  spacer. Prior to assembly, the inner surfaces of the glass plates were coated with a transparent, conductive layer of indium–tin–oxide and a rubbed nylon 6/6 alignment layer to provide a planar alignment. The assembled devices were capillary filled with liquid crystal and sealed with an epoxy resin cement. This device was mounted so that the beam passed through the sample (Laue scattering geometry).

A square wave electric field was applied to the sample and a trigger pulse was used to gate the detector, ensuring

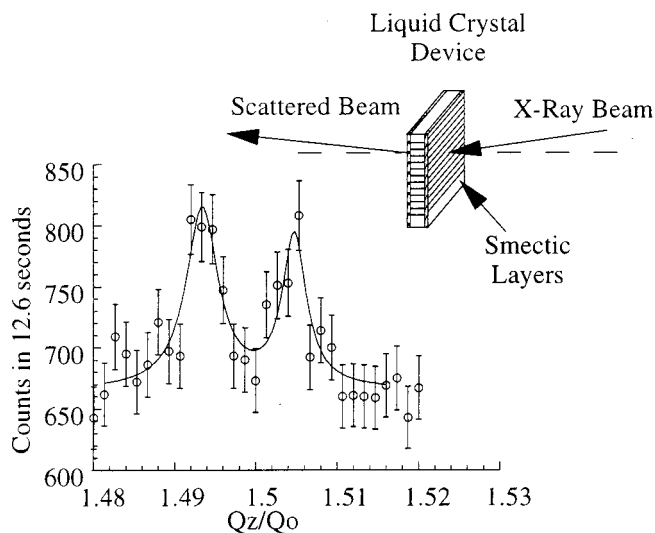


FIG. 3. Resonant peaks observed in the antiferroelectric phase in a device.

that data were collected only when a positive voltage was applied. The devices were mounted onto a Linkam hot stage that allowed temperature control of the device with a relative accuracy of  $\pm 0.05$  K. In the device the layers form a chevron structure as the sample is cooled into the  $\text{SmC}^*$  subphases.<sup>14,15</sup> In this study we concentrated on the antiferroelectric  $\text{SmC}^*$  phase. From previous studies, it is known that upon increasing the magnitude of the applied electric field, an antiferroelectric to ferroelectric phase transition is induced. It is also known<sup>16</sup> that, for relatively large electric fields, the chevron texture in antiferroelectric and ferroelectric devices evolves into a bookshelf texture in which the smectic layers are normal to the confining glass plates. Then, upon decreasing the applied field, the antiferroelectric phase returns oriented in a bookshelf texture. It is in this bookshelf texture that the antiferroelectric phase was measured.

To observe the smectic layer Bragg peaks, the sample was rocked into the Bragg condition. After maximizing the signal to noise ratio by shielding the detector and increasing the x-ray flux, a resonant signal was observed in the antiferroelectric phase at  $90.2^\circ\text{C}$  with no applied field. As was observed in the free-standing film sample [Fig. 2(b)], the  $Q_z/Q_o$  scan for the antiferroelectric phase in the device cell clearly shows splitting due to the helical pitch in the material (Fig. 3). From these data the pitch of the material inside the device was calculated to be  $0.61 \mu\text{m}$  at  $90.2^\circ\text{C}$ , comparable within the uncertainties of the curve fit to the data for the film.

On application of a 100 Hz square wave voltage of magnitude 40 V, the resonant antiferroelectric peaks vanished, confirming that the phase had been forced into a ferroelectric structure. The threshold for ferroelectric switching was found to be lower than 20 V. Further, no helical unwinding was observed on application of a field in the device geometry. This would have been evident from merging of the resonant antiferroelectric peaks, whereas no change in the peak positions occurred on application of the field.

Optical transmission studies of this device confirm that the threshold for ferroelectric switching is at 18.5 V (150 Hz) and that no unwinding occurs on application of a field below the antiferroelectric to ferroelectric switching threshold. Further, the x-ray measurements indicate that the chevron to bookshelf transition appears to coincide with the onset of the forced ferroelectric structure for this material and geometry.

This work describes the observation of resonant scattering at the Se edge in liquid crystal free-standing films and devices. The layer structures of the ferroelectric and antiferroelectric phases have been confirmed and a three-layer ferroelectric phase observed. The monotropic hexatic phase has been shown to have an antiferroelectric structure. By studying liquid crystal samples in a device cell, structural transitions can be deduced, e.g., helical unwinding and layer motions. The main advantage of studying the liquid crystal in a device cell is that structural changes which occur as part of the switching process can be directly observed. This experiment confirms that the application of an electric field to this material in the antiferroelectric phase does not change the helical pitch. Observations are also consistent with the transition from chevron to bookshelf structure, being coincident with the onset of ferroelectric switching in the device.

Work at the Advanced Photon Source was supported by the U.S. Department of Energy, Basic Energy Sciences, Office of Energy Research, under Contract No. W-31-109-ENG-38. L.S.M. thanks the Engineering and Physical Sciences Research Council for financial support.

<sup>1</sup>K. Miachi and A. Fukuda, *Handbook of Liquid Crystals*, (Wiley, VCH Verlag GmbH, 1998), Vol. 2B, Chap. VI (3) 3.3.1, p. 675.

<sup>2</sup>A. D. L. Chandani, Y. Ouchi, H. Takezoe, and A. Fukuda, *Jpn. J. Appl. Phys., Part 2* **28**, L1261 (1989).

<sup>3</sup>N. Yamamoto, N. Koshoubu, K. Mori, K. Nakamura, and Y. Yamada, *Ferroelectrics* **149**, 29 (1994).

<sup>4</sup>A. Fukuda, Y. Takahashi, T. Isozaki, K. Ishikawa, and H. Takezoe, *J. Mater. Chem.* **4**, 997 (1994).

<sup>5</sup>K. Hiraoka, T. Takahashi, K. Skarp, H. Takezoe, and A. Fukuda, *Jpn. J. Appl. Phys., Part 2* **30**, L1819 (1991).

<sup>6</sup>M. Cepic and B. Zeks, *Mol. Cryst. Liq. Cryst.* **263**, 61 (1995); V. L. Lorman, *ibid.* **262**, 437 (1995).

<sup>7</sup>P. Mach, R. Pindak, A. M. Levelut, P. Barois, H. T. Nguyen, C. C. Huang, and L. Furenlid, *Phys. Rev. Lett.* **81**, 1015 (1998).

<sup>8</sup>P. Mach, R. Pindak, A. M. Levelut, P. Barois, H. T. Nguyen, H. Baltes, M. Hird, K. Toyne, A. Seed, J. W. Goodby, C. C. Huang, and L. Furenlid, *Phys. Rev. E* **60**, 6793 (1999).

<sup>9</sup>J. Mills, R. Miller, and H. F. Gleeson, *Mol. Cryst. Liq. Cryst.* **303**, 145 (1997).

<sup>10</sup>J. T. Mills, H. F. Gleeson, M. Hird, P. Styring, and J. W. Goodby, *J. Mater. Chem.* **8**, 2385 (1998).

<sup>11</sup>V. E. Dmitrienko, *Acta Crystallogr., Sect. A: Found. Crystallogr.* **39**, 29 (1983).

<sup>12</sup>A. M. Levelut and B. Pansu, *Phys. Rev. E* **60**, 6803 (1999).

<sup>13</sup>K. Itoh, M. Kabe, K. Miyachi, Y. Takahashi, K. Ishikawa, H. Takezoe, and A. Fukuda, *J. Mater. Chem.* **7**, 40 (1997).

<sup>14</sup>T. P. Reiker, N. A. Clark, G. S. Smith, D. S. Parmar, E. B. Sirota, and C. R. Safinya, *Phys. Rev. Lett.* **59**, 2658 (1987).

<sup>15</sup>L. S. Matkin, L. Baylis, S. J. Watson, N. Bowring, H. F. Gleeson, A. Seed, M. Hird, and J. W. Goodby (unpublished).

<sup>16</sup>M. John, A. D. Chandani, Y. Ouchi, H. Takezoe, A. Fukuda, M. Ichihashi, and K. Furukawa, *Jpn. J. Appl. Phys., Part 2* **28**, L119 (1989).